AMERICAN JOURNAL OF PHYSIOLOGY
ENDOCRINOLOGY AND METABOLISM

Am J Physiol Endocrinol Metab 326: E215–E225, 2024.
First published December 20, 2023; doi:10.1152/ajpendo.00357.2023

RESEARCH ARTICLE

Immunometabolism

Monocyte immunometabolic reprogramming in human pregnancy: contribution of trophoblast cells

Fátima Merech,[1] Soledad Gori,[1] Guillermina Calo,[1] Vanesa Hauk,[1] Daniel Paparini,[1] Daiana Rios,[1] Brenda Lara,[1] Luciana Doga,[2] Luciana D'Eramo,[2] Aldo Squassi,[2] Rosanna Ramhorst,[1] Rafael J. Argüello,[3] Claudia Pérez Leirós,[1] and Daiana Vota[1]

[1]*Instituto de Química Biológica de la Facultad de Ciencias Exactas y Naturales (IQUIBICEN), Universidad de Buenos Aires (UBA)-Consejo Nacional de Investigaciones Científicas y Técnicas (CONICET), Buenos Aires, Argentina;* [2]*Facultad de Odontología, Cátedra de Odontología Preventiva y Comunitaria, Universidad de Buenos Aires (UBA), Buenos Aires, Argentina; and* [3]*Centre d'Immunologie de Marseille-Luminy, Aix Marseille University, CNRS, INSERM, Marseille, France*

Abstract

Immunometabolism research is uncovering the relationship between metabolic features and immune cell functions in physiological and pathological conditions. Normal pregnancy entails a fine immune and metabolic regulation of the maternal-fetal interaction to assist the energetic demands of the fetus with immune homeostasis maintenance. Here, we determined the immunometabolic status of monocytes of pregnant women compared with nonpregnant controls and its impact on monocyte anti-inflammatory functions such as efferocytosis. Monocytes from pregnant women (16–20 wk) and nonpregnant age-matched controls were studied. Single cell-based metabolic assays using freshly isolated monocytes from both groups were carried out in parallel with functional assays ex vivo to evaluate monocyte efferocytic capacity. On the other hand, various in vitro metabolic assays with human monocytes or monocyte-derived macrophages were designed to explore the effect of trophoblast cells in the profiles observed. We found that pregnancy alters monocyte metabolism and function. An increased glucose dependency and enhanced efferocytosis were detected in monocytes from pregnant women at resting states, compared with nonpregnant controls. Furthermore, monocytes display a reduced glycolytic response when stimulated with lipopolysaccharide (LPS). The metabolic profiling of monocytes at this stage of pregnancy was comparable with the immunometabolic phenotypes of human monocytes treated in vitro with human first trimester trophoblast cell conditioned media. These findings suggest that immunometabolic mechanisms are involved in the functional shaping of monocytes during pregnancy with a contribution of trophoblast cells. Results provide new clues for future hypotheses regarding pregnancies complicated by metabolic disorders.

NEW & NOTEWORTHY Immunometabolism stands as a novel perspective to understand the complex regulation of the immune response and to provide small molecule-based therapies. By applying this approach to study monocytes during pregnancy, we found that these cells have a unique activation pattern. They rely more on glycolysis and show increased efferocytosis/IL-10 production, but they do not have the typical proinflammatory responses. We also present evidence that trophoblast cells can shape monocytes into this distinct immunometabolic profile.

immunometabolism; monocytes; pregnancy; trophoblast soluble factors

INTRODUCTION

Immune and metabolic regulation of the maternal-fetal interaction characterizes early human pregnancy, assisting the energetic demands of the fetus with immune homeostasis maintenance. From embryo implantation until finishing placentation by about week 18, concurrent processes such as the sustained recruitment of circulating monocytes to the uterus, an extensive tissue remodeling, and increasing metabolic demands of placental cells challenge immune and metabolic homeostasis (1). Monocytes recruited to the pregnant uterus differentiate into M2-like decidual macrophages under the control of extravillous trophoblast cells (2, 3). Decidual macrophages contribute to vascular transformation, tissue repair, and to restore immune homeostasis through anti-inflammatory cytokine synthesis and the constant clearance of apoptotic bodies by efferocytosis (4). Various soluble factors released by trophoblast cells have been identified for their ability to

Correspondence: D. Vota (daiana_vota@qb.fcen.uba.ar); C. Pérez Leirós (cpleiros@qb.fcen.uba.ar).
Submitted 1 November 2023 / Revised 4 December 2023 / Accepted 18 December 2023

favor monocyte/macrophage recruitment, anti-inflammatory profiles, and efferocytosis at early stages and term of normal pregnancies (5–7). In line with this, defective placentation associates with altered immune, vascular, and trophoblast interaction, resulting in complicated pregnancies that threaten maternal and neonatal health and underlie metabolic programming of adult life (1, 3).

Over the past years, the novel standpoint of immunometabolism has emerged and contributed with new hypotheses to understand the regulation of the immune response and the fate of immune cells in health and disease (8–14). Metabolic reprogramming of monocytes and macrophages has been characterized in normal and pathologic conditions through newly developed single-cell approaches (15–18). High levels of glycolysis are a hallmark of inflammatory monocytes (17, 19) and also characterize tolerogenic dendritic cells (DCs) (20). Regarding pregnancy, differential metabolic reprogramming of human decidual macrophages in normal versus recurrent pregnancy loss has been recently reported using human first trimester placental samples and mouse pregnancy models (21, 22). However, the immunometabolic profiling of human maternal circulating monocytes during pregnancy has not been addressed so far, neither a conditioning role of trophoblast cell factors.

The aim of this work was to characterize the metabolic pathways active in circulating monocytes from pregnant women at 16–20 wk in basal and ex vivo lipopolysaccharide (LPS)-stimulated conditions and to deepen into the potential mechanisms of metabolic reprogramming induced by human first trimester trophoblast cells in vitro.

Using a recently developed "single-cell energetic metabolism by profiling translation inhibition" (SCENITH) method (17, 18, 20) suitable for human studies with small peripheral blood samples, and various classical metabolic and functional assays, we found that pregnancy reprograms monocyte metabolism to higher glucose dependency and reduced capacity of fatty acids and amino acids oxidation compared with monocytes from nonpregnant control women. This profile occurs in combination with a differential metabolic response upon LPS stimulation, since LPS-stimulated monocytes showed no changes in glycolytic and mitochondrial dependency in the pregnant group in contrast to the nonpregnant group where the characteristic higher glucose uptake and dependency was observed. The metabolic reprogramming of monocytes during pregnancy associates with higher efferocytosis than the nonpregnant group. Evidence supporting the contribution of trophoblast cell soluble factors to these differential metabolic and functional phenotypes is also presented.

MATERIALS AND METHODS

Patients

A population of 50 women (20–35 yr old) at their 16–20th week of pregnancy under regular obstetric control and age-matched nonpregnant women defined with similar social and epidemiological criteria participated in this study after signing an informed consent. Pregnant women with a diagnosis of hypertension, a body mass index (BMI) less than 18.5 or greater than 30 (WHO) before pregnancy, diabetics, with positive serology for syphilis, hepatitis B, Chagas disease, toxoplasmosis, HIV, and/or with antiphospholipid antibodies were excluded. Peripheral blood samples were obtained and metabolic and functional studies were carried out on monocytes ex vivo according to protocols approved by the Ethical Committee of the School of Dentistry (No. 20211157) and the Argentine Society of Clinical Investigation (SAIC 317). Informed consent was obtained from all subjects involved in the study.

Peripheral Blood Mononuclear Cells Purification and Monocyte Isolation

Blood samples (10 mL) of pregnant women or age-matched nonpregnant fertile volunteers were processed immediately for peripheral blood mononuclear cells (PBMCs) isolation through Ficoll Paque PLUS (GE Healthcare Cat. No. 17-1440-03). Monocytes from buffy coats of healthy women volunteers were isolated by Ficoll Paque PLUS and Percoll gradient (GE Healthcare, Cat. No. 17-5445-02) as described previously (23). Cell population purity (>80%) was checked by flow cytometry analysis with CD14 labeling as previously described (6, 24) in a FACS Aria II cytometer (BD Biosciences RRID:SCR_018091) using FlowJo software (FlowJo, RRID: SCR_008520, http://www.flowjo.com).

Human Monocyte-Derived Macrophages

Monocytes were cultured in RPMI-1640 medium (Thermo Fisher Scientific, Cat. No. 11875) supplemented with 10% fetal bovine serum (FBS, Internegocios No. FRA) and 50 ng/mL of human recombinant macrophage colony-stimulating factor (M-CSF, Miltenyi Biotec, Cat. No. 130-093-963) for 5 days leading to M0 macrophages.

SCENITH Analysis

SCENITH allows metabolic phenotyping of distinct cell subsets in the same sample and required a low number of cells. The SCENITH kit was obtained from http://www.scenith.com (18), and cells were treated following the PBMC protocol from the kit. PBMCs from 16 to 20th week of pregnancy or age-matched nonpregnant fertile women were stimulated ex vivo or not with 100 ng/mL of LPS (Sigma-Aldrich, Cat. No. L4391) for 20 min. After cell stimulation, cells were treated for 30–45 min at 37°C with DMSO (Control), 100 mM 2-deoxy-D-glucose (DG), 1 μM oligomycin (O), or a sequential combination of the drugs (DGO) at the final concentrations mentioned earlier. As a negative control, the translation initiation inhibitor harringtonine was added 15 min before addition of puromycin (puro) (harringtonine, 1 μg/mL). Puro (10 μg/mL) is added during the last 30 min of the metabolic inhibitors treatment. Then, cells were washed in cold PBS and stained with a combination of primary conjugated antibodies against surface markers for 25 min at 4°C in PBS 1×, 5% FBS, 2 mM EDTA (FACS wash buffer). After washing, cells were fixed and permeabilized using fixation and permeabilization buffer (Thermo Fisher Scientific Cat. No. 00-8222-49 and Cat. No. 00-8333-56) following manufacturer instructions. Intracellular staining of puro was performed incubating cells with a monoclonal antibody anti-puro Alexa Fluor 647 for 1 h at 4°C. Data was acquired in a FACS Aria II cytometer (BD Biosciences RRID:SCR_018091) and analyzed using FlowJo software (FlowJo, RRID:SCR_008520, http://www.flowjo.com). In the present work, we analyzed translation levels of CD14+

cells (eBiosciences, Cat. No. 25-0149-42). The metabolic CD14+ cells phenotyping is determined by analyzing the protein synthesis levels, measured as anti-puro mean fluorescence intensity (MFI), in cells cultured in the presence of DG or/and O metabolic inhibitors respect to control cells. Measurement of anti-puro MFI after addition of inhibitors allowed for the calculation of distinct metabolic parameters (Fig. 1*A*). Glucose and mitochondrial dependency: proportion of protein synthesis (measured as anti-puro MFI) dependent on glucose oxidation and oxidative phosphorylation (OXPHOS), respectively. Glycolytic capacity and fatty acid and/or amino acid oxidation (FAO/AAO) capacity indicate the maximum potential of cells to sustain protein synthesis when OXPHOS and glucose oxidation are inhibited, respectively (18).

Seahorse

Extracellular acidification rate (ECAR) was measured with the XF Extracellular Flux Analyzer [Seahorse, Agilent (RRID: SCR_013575)]. M0 human monocyte-derived macrophages (8.5×10^4) were placed in XFp cell culture microplates and stimulated for 18 h in RPMI-1640 supplemented with 2% FBS with or without 100 ng/mL LPS and/or trophoblast conditioned media (Tb-CM) obtained as described under *First Trimester-Derived Cell Conditioned Media*. Media was replaced for DMEM XF base (Millipore Sigma) supplemented with 2 mM glutamine (pH 7.4), and after 45 min at 37°C the plate was loaded into Seahorse XFp extracellular flux analyzer. ECAR was determined at the beginning of the assay and after the sequential addition of 10 mM D-glucose, 1 μM oligomycin, and 100 mM 2-DG. Values are expressed as mpH/min and were normalized to cell number obtained by *Incell* analysis directly after each run.

Glucose Uptake

Mouse anti-human CD14 PE (BD Biosciences Cat. No. 347497, RRID:AB_400312) was added for 20 min in 2% FBS in PBS at room temperature before or after stimulation with 100 ng/mL of LPS for 20 min or 18 h, respectively. Medium was removed and cells were incubated with 100 μM 2-NBDG (Thermo Fisher Scientific, Cat. No. N13195) for 5 min at 37°C, 5% CO_2 in glucose-free RPMI-1640 medium (Thermo Fisher Scientific, Cat. No. 11879). Cells were washed with cold PBS and resuspended in 2% FBS in PBS for flow cytometry analysis. Data were acquired in a FACS Aria II cytometer (BD Biosciences RRID:SCR_018091) and analyzed using FlowJo software (FlowJo, RRID:SCR_008520, http://www.flowjo.com).

Long-Chain Fatty Acids Uptake

Cells were stained and stimulated as for glucose uptake assay. BODIPY-FL C_{12} (Thermo Fisher Scientific, Cat. No. D3822) is a 12-carbon chain length saturated fatty acid linked to the fluorophore BODIPY (4,4-difluoro-3a,4a-diaza-s-indacene), resembling a 18-carbon fatty acid (25). The probe was preincubated with 0.1% fatty acid-free bovine serum albumin (FAF-BSA, Sigma-Aldrich, Cat. No. A8806) for 30 min at 37°C. Cells were washed twice with PBS and incubated with 5 μM BODIPY-FL C_{12} solution in serum-free RPMI-1640 for 5 min at 37°C, 5% CO_2. Cells were washed with 0.2% BSA, resuspended in 2% FBS in PBS solution, and data were acquired as for glucose uptake assay.

Efferocytosis of Autologous Apoptotic Neutrophils

Neutrophils were isolated from peripheral blood autologous samples by Ficoll-Hypaque gradients and subsequent Dextran purification (26). Spontaneous apoptotic neutrophils were obtained after 16-h incubation in RPMI-1640 and stained with carboxyfluorescein succinimidyl ester (CFSE) (Thermo Fisher Scientific Cat. No. 34554) as in the study by Vota et al. (24). The percentage of apoptosis was 50% as determined by annexin-propidium iodide staining (BD Biosciences Cat. No. 556547, RRID:AB_2869082) and flow cytometry detection. After isolation, monocytes (1×10^6) were cultured in 24-well polystyrene plates and conditioned for 20 h with RPMI-1640 10% FBS, w/wo 100 ng/mL of LPS. For metabolic pathways inhibition, 10 mM 2-DG (Sigma-Aldrich, Cat. No. D6134) and/or 100 nM rotenone (Sigma-Aldrich, Cat. No. R8875) were added to control cells 90 min before efferocytosis assay. Then, monocytes were challenged with apoptotic neutrophils in a 1:10 ratio. After 1 h of incubation, monocytes were washed with cold PBS, collected, stained with mouse anti-human CD14-PeCy7 antibody (Thermo Fisher Scientific Cat. No. 25-0149-42, RRID:AB_1582276), and the percentage of CD14/CFSE double positive cells was analyzed by flow cytometry, as described previously.

Lipid Droplets

Cells were treated as for glucose and LCFAs uptake, then washed twice with PBS and incubated with a 2 μM BODIPY 493/503 (Thermo Fisher Scientific, Cat. No. D3922) fluorescent probe in PBS for 15 min at 37°C and 5% CO_2. Cells were washed with cold PBS, harvested with EDTA 2 mM, supplemented with 2% FBS, resuspended in 2% FBS in PBS solution, and flow cytometry was performed as described earlier.

ELISA

IL-10 and IL-1β cytokines were evaluated in cell supernatants using commercial kits (BD Biosciences Cat. No. 555157, RRID:AB_2869031; BD Biosciences Cat. No. 557953, RRID:AB_2869109), according to the manufacturer's recommendations.

First Trimester Trophoblast-Derived Cell Conditioned Media

Trophoblast cells [First trimester human trophoblast cell lines Swan 71 (RRID:CVCL_D855) or HTR-8/SVneo (RRID: CVCL_7162)] were seeded in polystyrene plates until subconfluence as described previously (24). Medium was replaced to RPMI-1640 supplemented with 2% FBS and after 18 h of culture the conditioned media were collected, centrifuged to eliminate cell debris, and stored at −80°C.

Macrophage Phenotypic Markers Assessment by Flow Cytometry

Cells were stained with APC, PE, FITC, or PECy7-conjugated antibodies directed to surfer markers CD14 (BD Biosciences Cat. No. 555399, RRID:AB_398596; BD Biosciences Cat. No. 347497, RRID:AB_400312; Thermo Fisher Scientific, Cat. No. 25-0149-42, RRID:AB_1582276), CD86 [BioLegend Cat. No. 305406 (also 305405, 305438), RRID:AB_314526], CD209 (Thermo Fisher Scientific Cat. No. 17-2099-42, RRID:AB_11039758), and CD36

(BD Biosciences Cat. No. 555454, RRID:AB_2291112). Cells were recovered, washed with staining buffer, and incubated for 20 min at room temperature with antibodies in PBS supplemented with 2% FBS, then washed twice, and resuspended. Ten thousand events were acquired by flow cytometry and analyzed as described earlier.

RT-qPCR

Cellular messenger RNA (mRNA) was analyzed by RT-qPCR. Cells were treated as for glucose and LCFAs uptake. Total RNA was extracted using TriReagent according to the manufacturer's instructions. A total of 1 μg RNA was treated

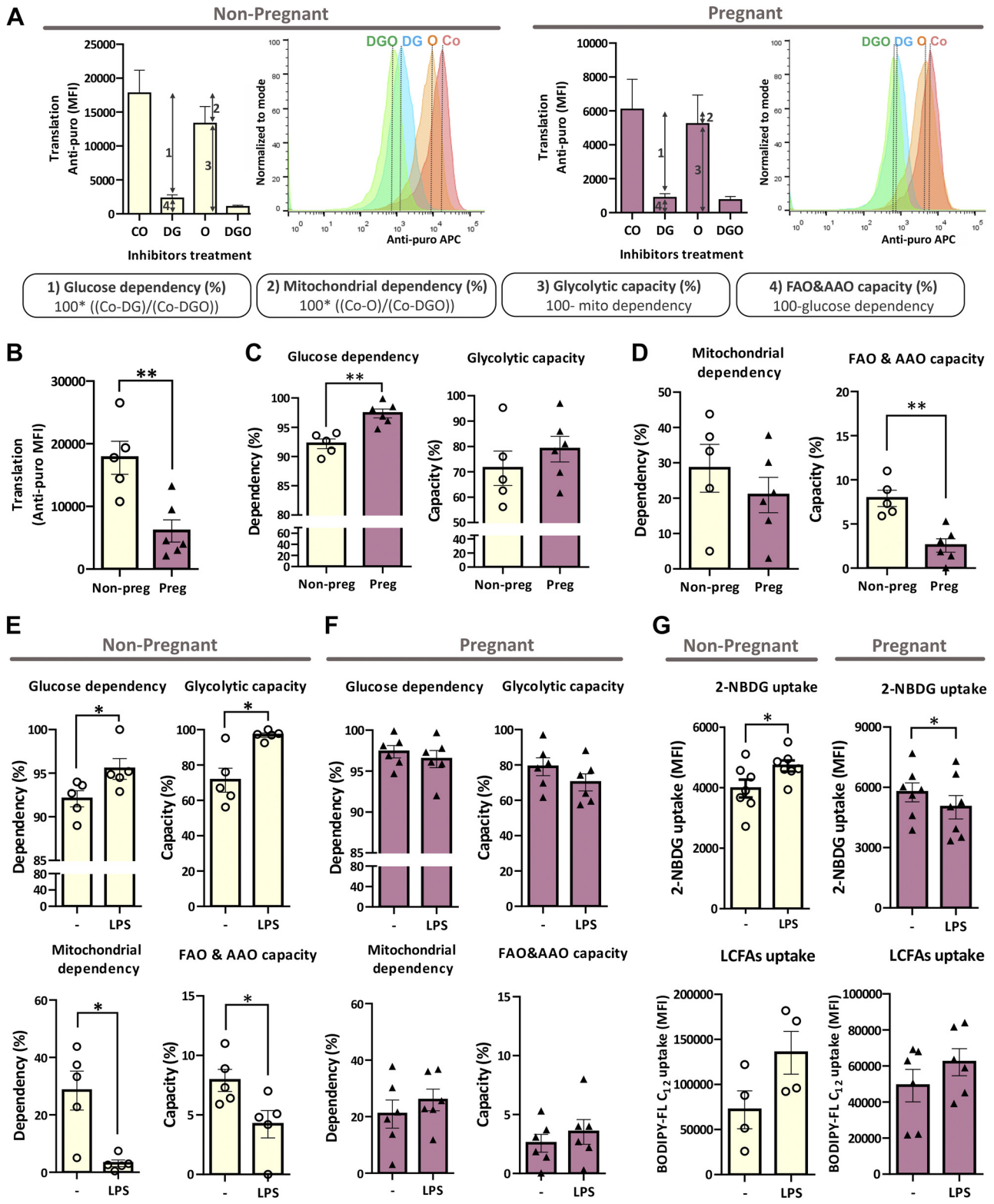

AJP-Endocrinol Metab • doi:10.1152/ajpendo.00357.2023 • www.ajpendo.org

with DNAse I to avoid DNA contamination, and the samples were reverse-transcribed using MMLV reverse transcriptase, RNAse inhibitor, and random primers (Promega, Cat. No. N2111). Complementary DNA (cDNA) was incubated with SYBR Green PCR Master Mix (Roche, Cat. No. 4913850001) and specific primers for *fatp2* (F: 5′-CACAGGTCTTCCAAAAGCAGC-3′, R: 5′-AGTCCGCAAGGCAAGAGTAG-3′) and *irg-1* (F: 5′TGCTGCTTTTGTGAACGGTG-3′, R: 5′ACTTTGGACTCCTTGGCAGG-3′) transcripts in a Bio-Rad iQ5 RT-PCR system (RRID:SCR_019721). Data were analyzed using $2^{-\Delta Ct}$ normalized to the endogenous gene control β2 microglobulin (F: 5′-AAGCAGCATCATGGAGGTTTG-3′, R: 5′-GAGCTACCTGTGGAGCAACC-3′).

Lactate Production

Lactate concentration in cell supernatant was measured 18 h after treatments with Accutrend Plus System (Roche), according to the manufacturer's instructions.

Mitochondrial Mass and Membrane Potential

Cells were washed twice and incubated with 250 nM MitoSpy Green (BioLegend Inc. Cat. No. 424805) and 250 nM MitoTracker CMXRos (Thermo Fisher Scientific, Cat. No. M46752) in FBS-free RPMI-1640 for 20 min at 37°C, 5% CO_2 for mitochondrial mass and membrane potential measurement, respectively. Cells were resuspended and flow cytometry was performed as described earlier. Membrane mitochondrial potential as the MFI was normalized to mitochondrial mass MFI and the ratio was depicted in the graph.

Statistical Analysis

Data were analyzed using GraphPad Prism 6 software (GraphPad Prism (RRID:SCR_002798) San Diego, CA) and Infostat software linked with R [(RRID:SCR_014310), FCA-UNC, Córdoba, Argentina]. Unpaired/paired Student's *t* test or RM/one-way ANOVA followed by Tukey's or Dunnett's multiple comparisons tests were used. When necessary, Welch's correction was used, or variances were modeled followed by least significant difference (LSD) Fisher's multiple comparisons test. Results are expressed as means ± SE. Differences between treatments were considered significant at $P < 0.05$.

RESULTS

Higher Glucose Dependency in Monocytes from Early Pregnant Women

We first assessed the profile of circulating monocytes from early pregnant women and nonpregnant controls in basal unstimulated conditions by single-cell metabolic analysis using SCENITH (18). The basis of this technique is that protein synthesis is tightly connected to ATP levels so, by analyzing the effect of metabolic inhibitors on fluorescent puromycin incorporation during protein translation, both glycolytic and mitochondrial dependency can be estimated by flow cytometry. High puromycin incorporation (displayed as median fluorescence intensity, MFI) was detected in monocytes from either nonpregnant or pregnant women, indicating measurable levels of protein synthesis in monocytes from freshly isolated PBMCs samples (Fig. 1*A*). Interestingly, monocytes from pregnant women showed lower levels of basal translation compared with nonpregnant women (Fig. 1*B*).

When the respective metabolic profiles were analyzed, a higher glucose dependency was observed in the pregnant group compared with the nonpregnant group (Fig. 1*C*). In parallel, monocytes from the pregnant group displayed lower capacity to use amino acids and fatty acids as fuels than monocytes from the nonpregnant, along with a trend to lower mitochondrial dependency (Fig. 1*D*). It is noteworthy that the glucose inhibitor 2-deoxy-D-glucose (DG) almost completely abolished the puromycin signal in all monocytes from pregnant women, indicating overall high glucose dependency (Fig. 1*A*). Inhibiting mitochondrial ATP production with oligomycin (O) had a milder effect (Fig. 1*A*).

When challenged ex vivo with a classical proinflammatory stimulus as LPS (100 ng/mL) to activate the immune response, monocytes from the nonpregnant control group increased their glucose dependence and also consistently increased their glycolytic capacity. LPS-stimulated monocytes ex vivo showed almost exclusive dependence on glucose for protein synthesis (Fig. 1*E*), whereas they decreased fatty acid and amino acid oxidation capacity (Fig. 1*E*), as expected (17, 18). In contrast, challenging monocytes from pregnant women with LPS did not increase their glucose dependency, neither their glycolytic capacity (Fig. 1*F*). Results obtained in monocytes stimulated with LPS using the SCENITH method were consistent with ex vivo assays carried out in paired samples to evaluate glucose or long-chain fatty acid uptake by flow cytometry using fluorescent probes (Fig. 1*G*).

Enhanced Efferocytosis in Monocytes from Pregnant Women

Based on the lack of metabolic reprogramming upon LPS stimulation in monocytes from pregnant women, we wondered whether other functions requiring energy such as efferocytosis and cytokine production are affected (27). First,

Figure 1. Monocytes from pregnant women display higher glucose dependency. Peripheral blood mononuclear cells (PBMCs) from pregnant women (16–20 wk) or age-matched nonpregnant fertile women were isolated as previously described, stimulated ex vivo or not with 100 ng/mL lipopolysaccharide (LPS), and single-cell energetic metabolism by profiling translation inhibition (SCENITH) analysis, 2-NBDG uptake or LCFAs uptake were performed by flow cytometry. *A*: translation levels measured as mean fluorescence intensity (MFI) of puromycin across samples untreated (Co) or treated with 2-deoxy-D-glucose (DG), oligomycin (O), or DG + oligomycin (DGO) inhibitors for nonpregnant (yellow) or pregnant (purpura) women. *Bottom*: calculations of metabolic SCENITH parameters. *B*: basal translation levels of monocytes from nonpregnant (white dots) vs. pregnant (black triangles) women. *C*: SCENITH parameters for glucose dependency and glycolytic capacity of cells from nonpregnant vs. pregnant women. *D*: SCENITH parameters for mitochondrial dependency and fatty acid and amino acid oxidative capacity of cells from nonpregnant vs. pregnant women. *E* and *F*: SCENITH parameters for cells from nonpregnant vs. pregnant women stimulated ex vivo or not with LPS 100 ng/mL. *G*: 2-NBDG and 4,4-difluoro-3a,4a-diaza-s-indacene (BODIPY)-FL C12 uptake of cells from nonpregnant or pregnant women stimulated or not with LPS 100 ng/mL. Results are expressed as means ± SE. Each point represents an individual sample. *$P < 0.05$, **$P < 0.01$, unpaired/paired Student's *t* test.

we explored efferocytosis by monocytes from both groups and the role of glycolysis. Figure 2*A* shows that monocytes from pregnant women engulfing autologous apoptotic cells have twice the efferocytic capacity of monocytes from the nonpregnant control. Interestingly, glucose metabolism inhibition with 2-DG reduced efferocytosis to a greater extent in monocytes from pregnant women compared with the control group (Fig. 2*B*). Moreover, rotenone, an inhibitor of mitochondrial electron transport chain, also reduced efferocytosis in the pregnant group (Fig. 2*B*). The inhibitory effect of rotenone was even higher in the presence of 2-DG in these monocytes (Fig. 2*B*, *right*), emphasizing the dependency on glucose associated to efferocytosis in monocytes at early pregnancy. We next tested whether LPS ex vivo stimulation of monocytes from pregnant women reduced their efferocytic capacity, a trait described for nonpregnant macrophages. Figure 2*C* shows that while this reduction is significant in monocytes in the nonpregnant group (Fig. 2*C*, *left*), efferocytosis remained unaffected in the pregnant group (Fig. 2*C*, *right*).

Figure 2, *D* and *E* shows pro- and anti-inflammatory cytokines IL-1β and IL-10 released to the supernatants of monocytes from pregnant and nonpregnant women. A higher IL-10 production was found in the pregnant versus the nonpregnant group, with no changes in IL-1β between groups (Fig. 2, *D* and *E*, *left*). LPS challenge the release of IL-10 and IL-1β in both groups (Fig. 2, *D* and *E*, *right*).

Trophoblast Cell Conditioned Media Prevent LPS-Induced Glucose Uptake and Promote Lipid Metabolism in Monocytes

Given the metabolic profiles observed in monocytes from pregnant women and the well-known role of trophoblast cells in shaping monocyte and macrophage functional phenotypes sustaining an anti-inflammatory milieu at early pregnancy (3, 24, 28–30), we tested the hypothesis that trophoblast cells also can reprogram the metabolic profiling of maternal monocytes and macrophages at the maternal-fetal interface. Using an in vitro design, we started characterizing rapid (20 min) glucose uptake in basal and LPS-stimulated conditions in monocytes treated or not with trophoblast cell conditioned media (Fig. 3, *A* and *B*). As shown in Fig. 3*B*, the conditioned media from first trimester trophoblast-derived cell line Swan 71 (Tb-CM) had no effect on the fluorescent glucose analogue 2-NBDG uptake, but it completely prevented glucose uptake in LPS-stimulated monocytes in this short period. The effects were identical to those obtained with another first trimester trophoblast cell line, HTR-8/SVneo (Supplemental Fig. S1). The lack of response to LPS in the presence of Tb-CM persisted when the uptake of glucose was analyzed after 18 h of incubation with LPS (Fig. 3*C*).

Interestingly, a differential modulation of lipids metabolism was observed in Tb-CM cultured monocytes (Fig. 3, *D*–*G*). Tb-CM alone promoted the uptake of long-chain fatty

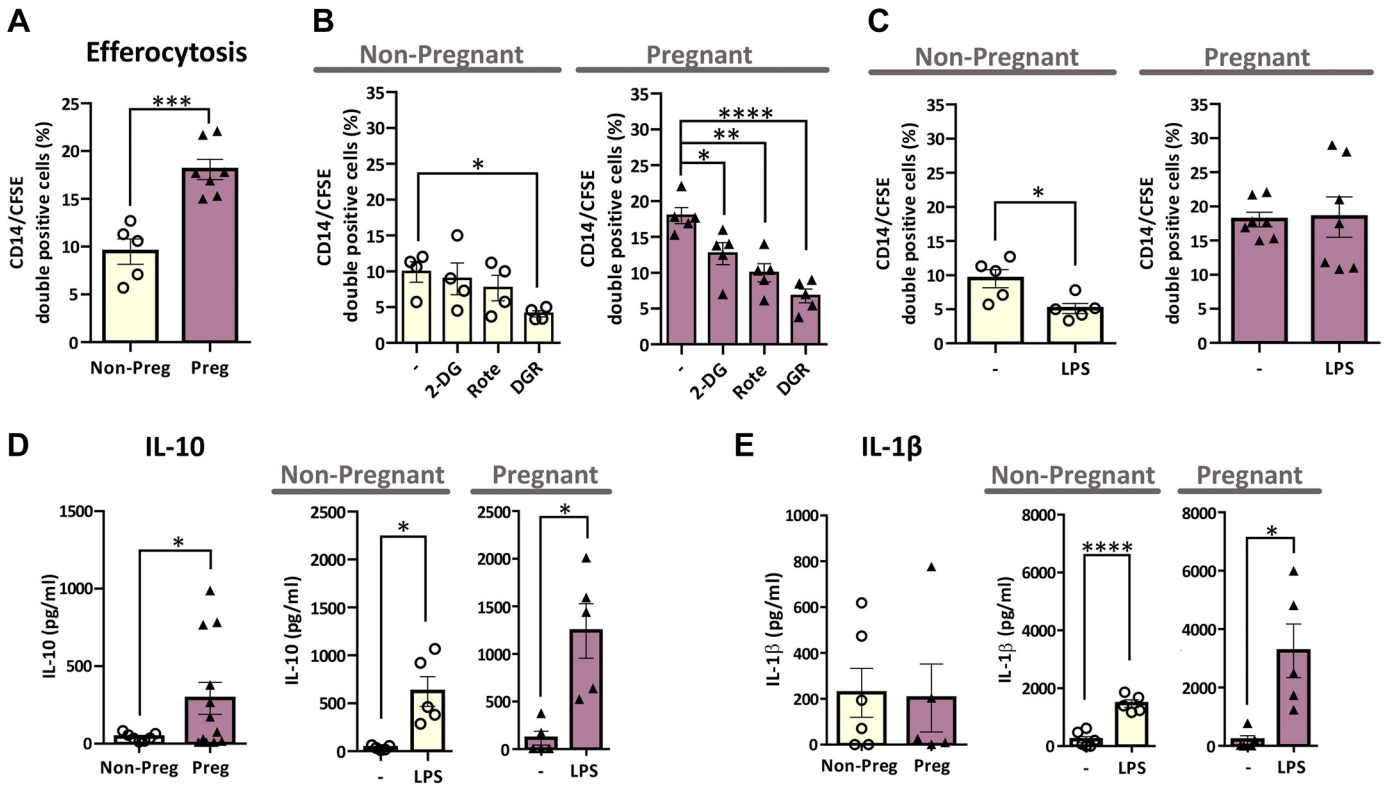

Figure 2. Monocytes from pregnant women show higher efferocytosis and IL-10 secretion. *A*–*C*: peripheral blood mononuclear cells (PBMCs) were cultured in polystyrene plates and conditioned or not with 100 ng/mL lipopolysaccharide (LPS). For metabolic pathways inhibition, 10 mM 2-deoxy-D-glucose (2-DG), 100 nM rotenone (Rote), or both (DGR) were added 90 min before efferocytosis assay. Monocytes were challenged with autologous apoptotic neutrophils stained with CFSE, and the percentage of CD14/CFSE double positive cells was analyzed by flow cytometry. IL-10 (*D*) and IL-1β (*E*) secretion by ELISA. Results are expressed as means ± SE. Each point represents an individual sample of monocytes from nonpregnant (white dots) or pregnant (black triangles) women. $^{*}P < 0.05$, $^{**}P < 0.01$, $^{***}P < 0.001$, $^{****}P < 0.0001$, unpaired/paired Student's *t* test with or without Welch's correction or ANOVA followed by Tukey's multiple comparisons test.

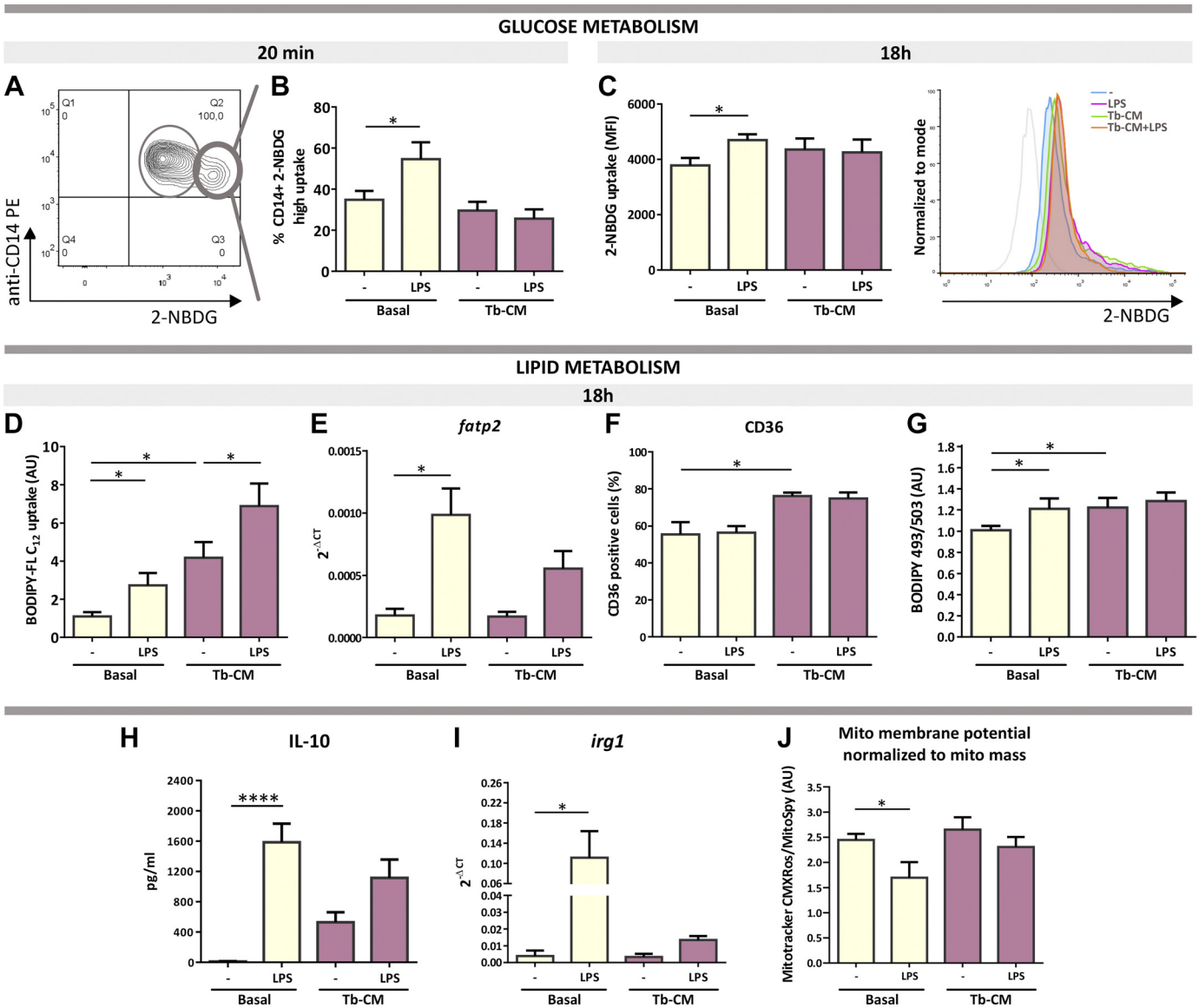

Figure 3. Trophoblast cell conditioned media prevent lipopolysaccharide (LPS)-induced glucose uptake and promote lipid metabolism in monocytes. Purified monocytes from nonpregnant women were incubated or not with Swan 71 trophoblast cells conditioned media (Tb-CM) and challenged or not with LPS for 20 min (*B*) or 18 h (*C*–*J*). Cells purified from 3 to 9 donors were incubated with 2-NBDG (*A*–*C*), 4,4-difluoro-3a,4a-diaza-s-indacene (BODIPY) FL C12 (*D*), BODIPY 493/503 (*G*), Mitotracker CMXRos or Mitospy (*J*) probes or mouse anti-human CD36 (*F*) and were analyzed by flow cytometry. Monocyte mRNA were obtained and analyzed by RT-qPCR (*E* and *I*) and monocyte conditioned media were collected after 18 h for IL-10 determination by ELISA (*G*). Values are means ± SE of at least three independent assays. $*P < 0.05$, $****P < 0.0001$. RM/one-way ANOVA followed by Tukey's multiple comparisons test.

acids whereas the effect of Tb-CM and LPS together was even higher (Fig. 3*D*, Supplemental Fig. S1). These results suggest a metabolic switch to higher fatty acid metabolism that paralleled the reduced glucose uptake promoted by Tb-CM upon LPS stimulation, an effect that was also seen for their specific transporter FATP2 (Fig. 3*E*). Tb-CM also induced a significant increase in the percentage of CD36 positive cells, a key fatty acid transporter, whereas LPS had no effect in either case (Fig. 3*F*). Of note, similar enhanced lipid droplet accumulation was observed with Tb-CM alone whereas there was no additional accumulation with LPS (Fig. 3*G*).

Similar to what we observed in monocytes from pregnant women (Fig. 2*D*), monocytes conditioned with Tb-CM showed a trend to higher IL-10 production versus basal values as well as upon LPS stimulation (Fig. 3*H*). On the basis that part of the effects of LPS and other proinflammatory stimuli on monocyte and macrophage metabolic reprogramming relies on induced Irg-1 enzyme expression that affects TCA performance (31), we explored its expression in our settings. Figure 3*I* shows that Tb-CM completely abolished the effect of LPS on Irg-1 expression. Finally, we evaluated the mitochondrial potential and mass in monocytes challenged with LPS for 18 h in basal conditions or in the presence of Tb-CM. Mitochondrial membrane potential was assessed by flow cytometry and normalized to mitochondrial mass. LPS induced an increase in the mitochondrial mass that was not associated to increased mitochondrial potential resulting in a lower ratio of these parameters that suggest mitochondrial

dysfunction (Fig. 3*J*). However, when monocytes were stimulated in the presence of Tb-CM this effect was not observed.

Trophoblast Cell Conditioned Media Inhibit LPS-Induced Glycolysis in Macrophages

Results from Figs. 1 and 3 indicate that in monocytes from pregnant women or in those conditioned with trophoblast factors, LPS failed to skew metabolism to glycolytic pathways as canonically described and observed in the control cells here. So taking into account that monocytes are recruited to the decidua and differentiated to M2-like macrophage phenotypes (5, 24, 28), the next question arising was whether macrophage metabolism was also conditioned by trophoblast factors. Figure 4, *A–C* confirms the same metabolic bias in macrophages as observed in monocytes to lowering LPS-induced glycolytic pathways with Tb-CM (Fig. 3). In fact, Tb-CM not only reduced LPS-induced glucose uptake (Fig. 4*A* and Supplemental Fig. S2) but also inhibited the increase in extracellular acidification rate induced by LPS as measured with the Seahorse assay (Fig. 4*B*). Moreover, LPS did not increase lactate release in the presence of Tb-CM (Fig. 4*C*) and instead favored long-chain fatty acid uptake (Fig. 4*D*). Interestingly, Tb-CM alone slightly increased extracellular flux suggesting higher glycolytic metabolism respect to basal macrophages, comparable with the observed higher glucose dependency in monocytes from pregnant versus nonpregnant women (Fig. 1 and Fig. 4, *B* and *C*). Finally, the phenotype of macrophages conditioned by Tb-CM and the effect of Tb-CM on LPS challenge were analyzed. Figure 4, *E* and *F* shows that macrophages stimulated with LPS in the presence of Tb-CM presented a lower increase of CD14/CD86 positive cells compared with LPS alone (Fig. 4*E*), similar to another proinflammatory signal as IL-1β (Fig. 4*F*). On the other hand, the percentage of CD209 positive cells was increased upon Tb-CM alone (Fig. 4*G*) and a similar trend was seen in IL-10 production (Fig. 4*H*), confirming the conditioning role of trophoblast cells to induce an M2-like phenotype in macrophages in these settings as previously shown (5). Furthermore, CD209 in the presence of Tb-CM remained unchanged upon LPS stimulation (Fig. 4*G*) and a limited response was seen in IL-10 compared with LPS in the basal conditions without Tb-CM (Fig. 4*H*).

DISCUSSION

The emerging field of immunometabolism is uncovering the relationship between metabolic features and functionality of immune cells. Several reports have revealed that macrophages are metabolically plastic cells that can distinctly tailor their cellular metabolism, depending on the stimulus or signal from the microenvironment, to facilitate their immune-promoting or resolving functions.

Successful pregnancy entails the constant profiling of maternal monocytes and monocyte-derived macrophages for adequate immune and proresolving responses with homeostasis maintenance. Most of the studies on monocytes during pregnancy have focused on the third trimester and not many studies evaluated monocyte profiles during the course of pregnancy (32, 33): a progressive phenotypical activation of monocytes from the first to the third trimester has been reported. So far, there are no reports on the immunometabolic status of circulating monocytes during pregnancy and its impact on monocyte anti-inflammatory functions such as efferocytosis.

Using multiple approaches ex vivo and in vitro using the SCENITH assay and the extracellular flux assay (Seahorse), among other metabolism and phenotyping techniques, evidence presented here shows that 16–20 wk' pregnancy reprograms monocyte metabolism to higher glucose dependence, a tendency to higher glycolytic capacity and lower global metabolic activity in basal conditions. In addition, it reduces glycolytic switch upon LPS stimulation. Single-cell metabolic analysis of monocytes from pregnant women reveals higher glycolytic, reduced fatty acid, and amino acid oxidation capacity, along with a decreased response to LPS (Fig. 1). These findings align with functional data of efferocytosis ex vivo (Fig. 2) and with data obtained by extracellular flux analysis and other complementary techniques in in vitro designs with human first trimester trophoblast conditioned media (Figs. 3 and 4).

Immune homeostasis maintenance is a feature of normal pregnancy (3). Enhanced proinflammatory signals and perturbed clearance of apoptotic bodies in circulation and in the pregnant uterus may contribute to the loss of homeostasis during placentation and the onset of pregnancy complications like hypertensive disorders and preeclampsia (29, 34). Thus, it is noteworthy that even with higher dependency on glycolysis in basal nonstimulated conditions, glycolytic pathways of monocytes from 16 to 20 wk pregnant were not boosted in response to a proinflammatory stimulus like LPS as seen in the nonpregnant control cells. The failure of LPS to further increase glycolysis in these monocytes could be related to their already elevated glucose dependency. However, a differential expression or signaling of LPS receptor cannot be ruled out. Furthermore, monocytes rewired to higher glycolytic dependency during pregnancy, and unfit to escalate glycolysis upon LPS challenge, display higher efferocytosis and anti-inflammatory IL-10 production, suggesting differential metabolic regulation of these processes. Of note, similar results were observed in tolerogenic DCs where tolerogenic signals increase glycolysis (17). Moreover, this observation is consistent with recent reports on human monocyte-derived macrophages (27, 35, 36). Efferocytosis in human phagocytes exposed to apoptotic Jurkat T lymphocytes for 1–6 h relies on glycolysis (27, 35). A distinction between the glycolysis induced by efferocytosis and the type of glycolysis that occurs when cells are proinflammatory stimulated with LPS was highlighted. Certainly, in our present settings, the higher efferocytosis observed in monocytes from pregnant women faced to autologous apoptotic neutrophils for 1–2 h was completely prevented by glucose oxidation metabolic inhibitors.

Regarding mitochondrial dependency, in monocytes from the nonpregnant group, fatty acid and amino acid oxidation capacity as well as mitochondrial dependency followed the expected reduction upon LPS stimulation. This was not the case in monocytes from 16 to 20 wk' pregnant women where a reduced capacity to oxidize fatty acids and amino acids was seen compared with the nonpregnant group in basal conditions. These parameters persisted unchanged within

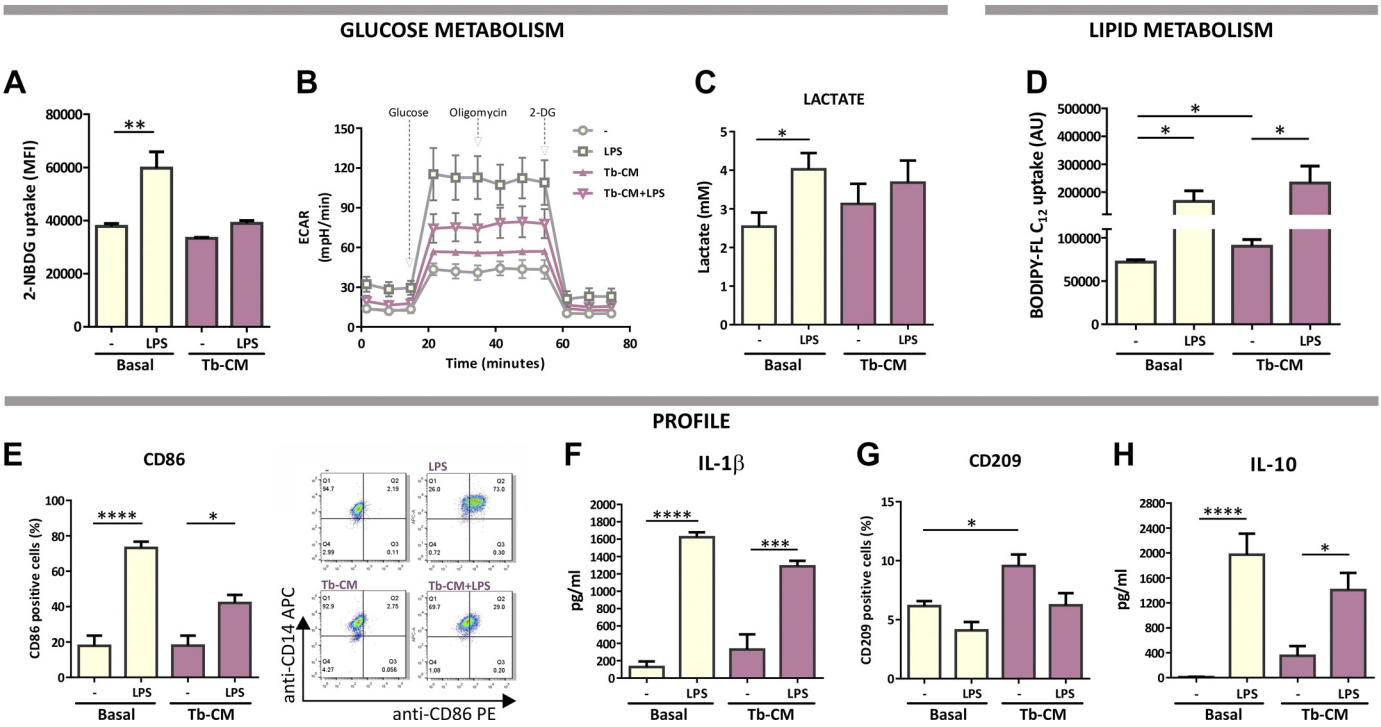

Figure 4. Trophoblast cell conditioned media inhibit lipopolysaccharide (LPS)-induced glycolysis in macrophages. Monocyte-derived macrophages from nonpregnant women were incubated or not with Swan 71 trophoblast cells conditioned media (Tb-CM) and challenged or not with LPS for 18 h. *A* and *D*: cells were incubated with 2-NBDG or 4,4-difluoro-3a,4a-diaza-s-indacene (BODIPY) FL C12 and analyzed by flow cytometry. Values are means ± SE of three independent assays. *B*: monocyte-derived macrophages were seeded in a Seahorse XFp analyzer, treated 18 h with LPS, Tb-CM or both and real-time extracellular acidification rate (ECAR) was determined during sequential treatments as indicated and expressed in mpH/min normalized to cell number. Means ± SE of two individual experiments. *C*: lactate production was determined by Accutrend Plus System ($n = 7$). *E* and *G*: macrophages were incubated with CD14, CD86, or CD209 and positive cells were analyzed by flow cytometry ($n = 4$). Macrophages' conditioned media from at least three donors were collected for IL-10 and IL-1β determination by ELISA (*F* and *H*). $^{*}P < 0.05$, $^{**}P < 0.01$, $^{***}P < 0.001$, $^{****}P < 0.0001$, RM/one-way ANOVA followed by Tukey's or least-significant different (LSD) Fisher's multiple comparisons test.

the pregnant group in the presence of LPS reflecting the metabolic bias to glycolysis referred earlier. Regarding fatty acid oxidation, LCFAs metabolism in monocytes and macrophages not only contribute to ATP production by β oxidation in mitochondria, but they also likely contribute to controlling the balance between pro- and anti-inflammatory mediators release (37). It is worth noting that in human monocytes with reduced mitochondrial dependency, LCFAs uptake seems not to fuel fatty acid oxidation, instead, their conversion into bioactive lipids mediators is suggested. Finally, lower translation levels were observed in monocytes from pregnant versus nonpregnant women in the resting state. Selective translational control appears as a major mechanism for regulating immune cell functions in both the adaptive and innate responses (38). Identifying regulatory components and transcription factors involved in monocytes' translational control and how they modulate monocyte immunological responses during pregnancy are a matter of future studies.

For many years, the lack of a maternal immune response against the allogeneic fetus has prompted the idea of pregnancy as an immunosuppression status. However, both inflammation and the consequent immunoregulatory mechanisms are critical for normal pregnancy so, a more dynamic concept has emerged which also explains the differential susceptibility of pregnant women to infectious diseases or to developing more severe responses to certain pathogens (3, 39). Thus, pregnancy evolves through three immune stages that not necessarily align with the trimesters: a first proinflammatory environment allows implantation and placentation, then by week 13 shifts to a second long-lasting period with an anti-inflammatory predominant profile that ensures complete placentation and fetal growth, and a short final shift back to a proinflammatory phase associated to labor. The immunometabolic reprogramming and efferocytosis profile of 16–20 wk' monocytes shown here is consistent with their role in the anti-inflammatory fetal growing stage.

This immune cooperation between the maternal immune system and the placenta throughout pregnancy relies on trophoblast cells (3). Considering that first trimester cytotrophoblast cells integrate metabolic and immune signals and release soluble factors that control monocyte and macrophage functional phenotypes (3, 5, 24), in vitro designs were carried out to deepen into the mechanisms of monocyte/macrophage metabolic reprogramming at early pregnancy. When challenged with LPS, both monocytes and macrophages conditioned with first trimester human trophoblast media failed to reprogram their metabolism to higher glucose uptake, lactate release, and extracellular acid flux. This inhibitory effect of trophoblast factors on glycolytic pathways was consistent with an M2-like predominant profile induced in macrophages as shown here and described previously (5, 24). On the other hand, lipid metabolism studied through fatty acid uptake and lipid droplet accumulation

was increased by the trophoblast medium alone in monocytes and it was even higher after LPS challenge. Moreover, Tb-CM increased the number of CD36 positive monocytes that was not modified by LPS challenge. This type 2 cell surface scavenger receptor widely expressed in immune cells has a dual role acting as a signaling factor for apoptotic cell recognition and phagocytosis as well as a long-chain fatty acid transporter associated to an M2-like macrophage phenotype (40). Thus, trophoblast factors would contribute to anabolic rather than catabolic metabolism in monocytes and macrophages, in line with the anti-inflammatory and M2-like profiles observed and the enhanced efferocytosis reported previously (24). In normal pregnancy at term, a differential phenotype of monocytes in response to LPS and efferocytic function was reported, and the role of systemic and decidual factors was proposed (6, 41). Regarding monocyte efferocytosis capacity during pregnancy, it is increased at 16–20 wk in conditions of immune homeostasis as shown here, and it was reported lower at term compared with the nonpregnant, probably due to the proinflammatory milieu with increased acute-phase proteins wherein monocytes are exposed in the third trimester and shortly before delivery (42, 43). Monocytes from pregnant women at 20–39 wk of gestation were also analyzed for reactive oxygen species baseline levels or after challenged in vitro with another bacterial stimulus (fMLP) (43). An enhanced, although not maximal, oxidative burst was observed suggesting an activation state particular of normal pregnancy that differs from that observed in the course of an infection (43). The role of trophoblast-derived extracellular vesicles and/or specific soluble factors produced by trophoblast cells in the metabolic profiling of circulating monocytes remains to be investigated.

Most of the studies on monocytes during pregnancy focused on the third trimester and not many studies have evaluated monocyte profiles during the course of pregnancy (32). A progressive phenotypical activation of monocytes from the first trimester to the third trimester has been reported. Our present results add an immunometabolic perspective to previous work on monocytes from normal pregnancies, providing new clues to the understanding of the regulatory mechanisms that operate during pregnancy and finding future hypothesis regarding pregnancies complicated by placental insufficiency or metabolic disorders. Extending the present studies to groups of patients at risk of preeclampsia or gestational diabetes-complicated pregnancies could open the possibility that the immunometabolic profiling of circulating monocytes and/or the circulating levels of certain metabolites be part of the set of biomarkers currently used in the scanning and following up of these populations.

ETHICAL APPROVALS

The study was conducted in accordance with the Declaration of Helsinki and approved by the Ethics Committee of Argentine Society of Clinical Investigation Board for studies involving humans.

DATA AVAILABILITY

The data that support the findings of this study are available from the corresponding author upon reasonable request.

SUPPLEMENTAL DATA

Supplemental Fig. S1: https://doi.org/10.6084/m9.figshare.24712044.

Supplemental Fig. S2: https://doi.org/10.6084/m9.figshare.24714777.

ACKNOWLEDGMENTS

Authors thank Dr. Laura Morelli and Lorenzo Campanelli from the “Ultrasensitive analysis of mitochondrial respiration and glycolysis,” STAN-CONICET. We are grateful to all the nonpregnant and pregnant women who accepted to participate in the protocols.

GRANTS

This work was supported by Agencia Nacional de Promoción Científica y Tecnológica Grants PICT 2021-I-A-00318 and PICT 2019-1554 (to C.P.L.); PICT 2018-2584 and PICT 2021/00274 (to D.V.), Universidad de Buenos Aires Grant UBACyT 20020170100317BA, and Consejo Nacional de Investigaciones Científicas y Técnicas (CONICET) Grant PIBAA28720211010 1109CO (to D.V.), Buenos Aires, Argentina. We also acknowledge Agence Nationale de la Recherche (ANR) Grant ANR-20-CE-CE14-0028-01 (to R.J.A.).

DISCLOSURES

No conflicts of interest, financial or otherwise, are declared by the authors.

AUTHOR CONTRIBUTIONS

C.P.L. and D.V. conceived and designed research; F.M., S.G., G.C., V.H., D.P., D.R., B.L., L.D., L.D., and D.V. performed experiments; F.M. and D.V. analyzed data; A.S., R.J.A., C.P.L., and D.V. interpreted results of experiments; F.M. prepared figures; C.P.L. and D.V. drafted manuscript; R.R., R.J.A., C.P.L., and D.V. edited and revised manuscript; F.M., S.G., G.C., V.H., D.P., D.R., B.L., L.D., L.D., A.S., R.R., R.J.A., C.P.L., and D.V. approved final version of manuscript.

REFERENCES

1. **Aplin JD**, **Myers JE**, **Timms K**, **Westwood M.** Tracking placental development in health and disease. *Nat Rev Endocrinol* 16: 479–494, 2020. doi:10.1038/s41574-020-0372-6.
2. **Chambers M**, **Rees A**, **Cronin JG**, **Nair M**, **Jones N**, **Thornton CA.** Macrophage plasticity in reproduction and environmental influences on their function. *Front Immunol* 11: 607328, 2020. doi:10.3389/fimmu.2020.607328.
3. **Mor G**, **Aldo P**, **Alvero AB.** The unique immunological and microbial aspects of pregnancy. *Nat Rev Immunol* 17: 469–482, 2017. doi:10.1038/nri.2017.64.
4. **Nagamatsu T**, **Schust DJD.** The contribution of macrophages to normal and pathological pregnancies. *Am J Reprod Immunol* 63: 460–471, 2010. doi:10.1111/j.1600-0897.2010.00813.x.
5. **Paparini DE**, **Choudhury RH**, **Vota DM**, **Karolczak-Bayatti M**, **Finn-Sell S**, **Grasso EN**, **Hauk VC**, **Ramhorst R**, **Pérez Leirós C**, **Aplin JD.** Vasoactive intestinal peptide shapes first-trimester placenta trophoblast, vascular, and immune cell cooperation. *Br J Pharmacol* 176: 964–980, 2019. doi:10.1111/bph.14609.
6. **Paparini D**, **Grasso E**, **Fernandez L. D C**, **Merech F**, **Weingrill-Barbano R**, **Correa-Silva S**, **Izbizky G**, **Abasolo JI**, **Hauk V**, **Ramhorst R**, **Bevilaqcua E**, **Pérez Leirós C.** Decidual factors and vasoactive intestinal peptide guide monocytes to higher migration, efferocytosis and wound healing in term human pregnancy. *Acta Physiol (Oxf)* 232: e13579, 2021. doi:10.1111/apha.13579.
7. **Ramhorst R**, **Grasso E**, **Vota D**, **Gori S**, **Hauk V**, **Paparini D**, **Calo G**, **Pérez Leirós C.** From decidualization to pregnancy progression: an

overview of immune and metabolic effects of VIP. *Am J Reprod Immunol* 88: e13601, 2022. doi:10.1111/aji.13601.
8. **Mathis D**, **Shoelson SE.** Immunometabolism: an emerging frontier. *Nat Rev Immunol* 11: 81–83, 2011. doi:10.1038/nri2922.
9. **O'Neill LAJ**, **Kishton RJ**, **Rathmell J.** A guide to immunometabolism for immunologists. *Nat Rev Immunol* 16: 553–565, 2016. doi:10.1038/nri.2016.70.
10. **Man K**, **Kutyavin VI**, **Chawla A.** Tissue immunometabolism: development, physiology, and pathobiology. *Cell Metab* 25: 11–26, 2018. doi:10.1016/j.cmet.2016.08.016.
11. **Patel CH**, **Leone RD**, **Horton MR**, **Powell JD.** Targeting metabolism to regulate immune responses in autoimmunity and cancer. *Nat Rev Drug Discov* 18: 669–688, 2019. doi:10.1038/s41573-019-0032-5.
12. **Jenkins BJ**, **Rees A**, **Jones N**, **Thornton CA.** Does altered cellular metabolism underpin the normal changes to the maternal immune system during pregnancy? *Immunometabolism* 3: e210031, 2021. doi:10.20900/immunometab20210031.
13. **Voss K**, **Hong HS**, **Bader JE**, **Sugiura A**, **Lyssiotis CA**, **Rathmell JC.** A guide to interrogating immunometabolism. *Nat Rev Immunol* 21: 637–652, 2021. doi:10.1038/s41577-021-00529-8.
14. **Maher AK**, **Burnham KL**, **Jones EM**, **Tan MMH**, **Saputil RC**, **Baillon L**, **Selck C**, **Giang N**, **Argüello R**, **Pillay C**, **Thorley E**, **Short C-E**, **Quinlan R**, **Barclay WS**, **Cooper N**, **Taylor GP**, **Davenport EE**, **Dominguez-Villar M.** Transcriptional reprogramming from innate immune functions to a pro-thrombotic signature by monocytes in COVID-19. *Nat Commun* 13: 7947, 2022. doi:10.1038/s41467-022-35638-y.
15. **Van den Bossche J**, **O'Neill LA**, **Menon D.** Macrophage immunometabolism: where are we (going)? *Trends Immunol* 38: 395–406, 2017. doi:10.1016/j.it.2017.03.001.
16. **Artyomov MN**, **Van den Bossche J.** Immunometabolism in the single-cell era. *Cell Metab* 32: 710–725, 2020. doi:10.1016/j.cmet.2020.09.013.
17. **Verberk SGS**, **de Goede KE**, **Gorki FS**, **van Dierendonck XAMH**, **Argüello RJ**, **Van den Bossche J.** An integrated toolbox to profile macrophage immunometabolism. *Cell Rep Methods* 2: 100192, 2022. doi:10.1016/j.crmeth.2022.100192.
18. **Argüello RJ**, **Combes AJ**, **Char R**, **Gigan J-P**, **Baaziz AI**, **Bousiquot E**, **Camosseto V**, **Samad B**, **Tsui J**, **Yan P**, **Boissonneau S**, **Figarella-Branger D**, **Gatti E**, **Tabouret E**, **Krummel MF**, **Pierre P.** SCENITH: a flow cytometry-based method to functionally profile energy metabolism with single-cell resolution. *Cell Metab* 32: 1063–1075.e7, 2020. doi:10.1016/j.cmet.2020.11.007.
19. **Galvain Peña S**, **ÓNeill LAJ.** Metabolic reprograming in macrophage polarization. *Front Immunol* 5: 420, 2014. doi:10.3389/fimmu.2014.00420.
20. **Adamik J**, **Munson PV**, **Hartmann FJ**, **Combes AJ**, **Pierre P**, **Krummel MF**, **Bendall SC**, **Argüello RJ**, **Butterfield LH.** Distinct metabolic states guide maturation of inflammatory and tolerogenic dendritic cells. *Nat Commun* 13: 5184, 2022. doi:10.1038/s41467-022-32849-1.
21. **Gao L**, **Xu Q-H**, **Ma L-N**, **Luo J**, **Muyayalo KP**, **Wang L-L**, **Huang D-H**, **Xiao X-J**, **Cheng S-B**, **Mor G**, **Liao A-H.** Trophoblast-derived lactic acid orchestrates decidual macrophage differentiation via SRC/LDHA signaling in early pregnancy. *Int J Biol Sci* 18: 599–616, 2022. doi:10.7150/ijbs.67816.
22. **Sheng Y**, **Hu W**, **Shen H-H**, **Wei C**, **Liu Y**, **Ma X-Q**, **Li M-Q**, **Zhu X.** An imbalance of the IL-33/ST2-AXL-efferocytosis axis induces pregnancy loss through metabolic reprogramming of decidual macrophages. *Cell Mol Life Sci* 79: 173, 2022. doi:10.1007/s00018-022-04197-2.
23. **Gori S**, **Soczewski E**, **Fernández L**, **Grasso E**, **Gallino L**, **Merech F**, **Colado A**, **Borge M**, **Pérez Leirós C**, **Salamone G**, **Ramhorst R.** Decidualization process induces maternal monocytes to tolerogenic IL-10-producing dendritic cells (DC-10). *Front Immunol* 11: 1571, 2020. doi:10.3389/fimmu.2020.01571.
24. **Vota D**, **Paparini D**, **Hauk V**, **Toro A**, **Merech F**, **Varone C**, **Ramhorst R**, **Pérez Leirós C.** Vasoactive intestinal peptide modulates trophoblast-derived cell line function and interaction with phagocytic cells through autocrine pathways. *Sci Rep* 6: 26364, 2016. doi:10.1038/srep26364.
25. **Kolahi K**, **Louey S**, **Varlamov O**, **Thornburg K.** Real-time tracking of BODIPY-C12 long-chain fatty acid in human term placenta reveals unique lipid dynamics in cytotrophoblast cells. *PLoS One* 11: e0153522, 2016. doi:10.1371/journal.pone.0153522.
26. **Calo G**, **Sabbione F**, **Vota D**, **Paparini D**, **Ramhorst R**, **Trevani A**, **Leirós CP.** Trophoblast cells inhibit neutrophil extracellular trap formation and enhance apoptosis through vasoactive intestinal peptide-mediated pathways. *Hum Reprod* 32: 55–64, 2017. doi:10.1093/humrep/dew292.
27. **Morioka S**, **Perry JSA**, **Raymond MH**, **Medina CB**, **Zhu Y**, **Zhao L**, **Serbulea V**, **Onengut-Gumuscu S**, **Leitinger N**, **Kucenas S**, **Rathmell JC**, **Makowski L**, **Ravichandran KS.** Efferocytosis induces a novel SLC program to promote glucose uptake and lactate release. *Nature* 563: 714–718, 2018. doi:10.1038/s41586-018-0735-5.
28. **Fest S**, **Aldo PB**, **Abrahams VM**, **Visintin I**, **Alvero A**, **Chen R**, **Chavez SL**, **Romero R**, **Mor G.** Trophoblast-macrophage interactions: a regulatory network for the protection of pregnancy. *Am J Reprod Immunol* 57: 55–66, 2007. doi:10.1111/j.1600-0897.2006.00446.x.
29. **Tong M**, **Abrahams VM.** Immunology of the placenta. *Obstet Gynecol Clin North Am* 47: 49–63, 2020. doi:10.1016/j.ogc.2019.10.006.
30. **Paparini D**, **Grasso E**, **Calo G**, **Vota D**, **Hauk V**, **Ramhorst R**, **Leirós CP.** Trophoblast cells primed with vasoactive intestinal peptide enhance monocyte migration and apoptotic cell clearance through αvβ3 integrin portal formation in a model of maternal-placental interaction. *Mol Hum Reprod* 21: 930–941, 2015. doi:10.1093/molehr/gav059.
31. **Peace CG**, **O'Neill LA.** The role of itaconate in host defense and inflammation. *J Clin Invest* 132: e148548, 2022. doi:10.1172/JCI148548.
32. **Faas MM**, **de Vos P.** Maternal monocytes in pregnancy and preeclampsia in humans and in rats. *J Reprod Immunol* 119: 91–97, 2017. doi:10.1016/j.jri.2016.06.009.
33. **True H**, **Blanton M**, **Sureshchandra S**, **Messaoudi I.** Monocytes and macrophages in pregnancy: the good, the bad, and the ugly. *Immunol Rev* 308: 77–92, 2022. doi:10.1111/imr.13080.
34. **Abrahams VM**, **Kim YM**, **Straszewski SL**, **Romero R**, **Mor G.** Macrophages and apoptotic cell clearance during pregnancy. *Am J Reprod Immunol* 51: 275–282, 2004. doi:10.1111/j.1600-0897.2004.00156.x.
35. **Schilperoort M**, **Ngai D**, **Katerelos M**, **Power DA**, **Tabas I.** PFKFB2-mediated glycolysis promotes lactate-driven continual efferocytosis by macrophages. *Nat Metab* 5: 431–444, 2023. doi:10.1038/s42255-023-00736-8.
36. **Morioka S**, **Maueröder C**, **Ravichandran KS.** Living on the edge: efferocytosis at the interface of homeostasis and pathology. *Immunity* 50: 1149–1162, 2019. doi:10.1016/j.immuni.2019.04.018.
37. **Ménégaut L**, **Jalil A**, **Thomas C**, **Masson D.** Macrophage fatty acid metabolism and atherosclerosis: the rise of PUFAs. *Atherosclerosis* 291: 52–61, 2019. doi:10.1016/j.atherosclerosis.2019.10.002.
38. **Piccirillo CA**, **Bjur E**, **Topisirovic I**, **Sonenberg N**, **Larsson O.** Translational control of immune responses: from transcripts to translatomes. *Nat Immunol* 15: 503–511, 2014. doi:10.1038/ni.2891.
39. **Racicot K**, **Kwon JY**, **Aldo P**, **Silasi M**, **Mor G.** Understanding the complexity of the immune system during pregnancy. *Am J Reprod Immunol* 72: 107–116, 2014. doi:10.1111/aji.12289.
40. **Chen Y**, **Zhang J**, **Cui W**, **Silverstein RL.** CD36, a signaling receptor and fatty acid transporter that regulates immune cell metabolism and fate. *J Exp Med* 219: e20211314, 2022. doi:10.1084/jem.20211314.
41. **Farias-Jofre M**, **Romero R**, **Galaz J**, **Xu Y**, **Tao L**, **Demery-Poulos C**, **Arenas-Hernandez M**, **Bhatti G**, **Liu Z**, **Kawahara N**, **Kanninen T**, **Shaffer Z**, **Chaiworapongsa T**, **Theis KR**, **Tarca AL**, **Gomez-Lopez N.** Pregnancy tailors endotoxin-induced monocyte and neutrophil responses in the maternal circulation. *Inflamm Res* 71: 653–668, 2022. doi:10.1007/s00011-022-01569-z.
42. **Mor G**, **Cardenas I.** The immune system in pregnancy: a unique complexity. *Am J Reprod Immunol* 63: 425–433, 2010. doi:10.1111/j.1600-0897.2010.00836.x.
43. **Naccasha N**, **Gervasi MT**, **Chaiworapongsa T**, **Berman S**, **Yoon BH**, **Maymon E**, **Romero R.** Phenotypic and metabolic characteristics of monocytes and granulocytes in normal pregnancy and maternal infection. *Am J Obstet Gynecol* 185: 1118–1123, 2001. doi:10.1067/mob.2001.117682.